Joint Centre for Mesoscale Meteorology, Reading, UK

Sensitivity of short-range weather forecasts to local potential vorticity modifications

A. Thorpe
M. Demirtas

Internal Report No. 71

July 1997

Met Office Joint Centre for Mesoscale Meteorology Department of Meteorology
University of Reading PO Box 243 Reading RG6 6BB United Kingdom
Tel: +44 (0)118 931 8425 Fax: +44 (0)118 931 8791
www.metoffice.com

Designed and produced by the Met Office © Crown copyright 2001 01/0240 The Met Office logo is a registered trademark.

SENSITIVITY OF SHORT-RANGE WEATHER FORECASTS TO LOCAL POTENTIAL VORTICITY MODIFICATIONS

MERAL DEMIRTAS* and ALAN J. THORPE

JCMM#, Department of Meteorology, University of Reading, UK

* **Corresponding author address:** Dr. Meral Demirtas, JCMM, Department of Meteorology, University of Reading, Earley Gate, RG6 6BB, United Kingdom. E-mail: swrdemas@reading.ac.uk

The Joint Centre for Mesoscale Meteorology (JCMM) is supported by the UK Meteorological Office and the Department of Meteorology, University of Reading.

Abstract

The use of potential vorticity concepts to understand extra-tropical cyclones, anticyclones and fronts is important not only for reconciling theory with observations, but also for delineating measurements necessary to improve the accuracy of short range forecasts. As yet potential vorticity thinking has been insufficiently applied to weather forecasting. This report presents a new method, to use potential vorticity ideas by combining them with satellite water vapour imagery in a manner that has not been documented before. The aim of this method is to test sensitivity of short-range weather forecast to local potential vorticity modifications. It also aims to monitor incipient errors in short range weather forecasting and to provide dynamically consistent data to re-run potentially poor forecasts. By using PV concepts one can infer additional atmospheric flow and temperature data which cannot otherwise be simply derived from the water vapour data. In this way dynamical concepts add considerable value to the water vapour data which by themselves would probably not have as significant a forecast impact.

Case studies in which the new method is used shed light on how observations and dynamical concepts could be used together to improve our understanding and ability to forecast mid-latitude weather systems. In cases where the analysis errors occur at upper levels of the troposphere the method leads to a significant improvement in the short-range forecast skill. In general, it is useful in highlighting where forecast problems are arising.

1. INTRODUCTION

One of the central issues of meteorology concerns the understanding of, and ability to forecast, the behavior of mid-latitude weather systems. With the use of synoptic examples and sensitivity experiments, processes contributing to the rapid development of extratropical cyclones have been identified in the scientific literature. Lately, the discussions have been extended based on potential vorticity concepts. These give a vivid view of how on the one hand upper-level and low level processes, and on the other hand physical and dynamical processes, interact with each other during cyclonic developments.

The advantages of potential vorticity (hereafter PV) concepts to describe and understand atmospheric dynamics occur due to two main properties of PV which are its conservation and its invertibility (Hoskins et al. 1985). The conservation property enables one to identify and follow significant features in space and time, if the air flow is both frictionless and dry adiabatic. This is a good approximation for short time intervals and for air-flows away from the Earth's surface and clouds. In physical terms conservation of potential vorticity can be thought as combining the first law of thermodynamics for dry adiabatic motion with the conservation of angular momentum. The invertibility property is an important tool, allowing one to quantify the importance of PV features in terms of the strength of their associated circulations and temperature patterns so that their capacity to enhance the development of other features can be assessed (Davis and Emanuel 1991, and Thorpe and Bishop 1995). It could also be particularly useful in providing dynamically consistent wind and temperature data to initialise numerical weather forecasts.

Dynamically meaningful information can be illustrated on a single PV chart by displaying PV distributions on isentropic surfaces. In practice, a suitable isentropic surface for viewing PV is one that intersects the polar front jet since the anomalies responsible for many atmospheric developments are visible there. Such an isentrope will be in the lower troposphere in the sub-tropics and will rise through the polar front emerging in the lower stratosphere on the poleward side of the jet. In this study, the 315K isentropic surface is used for winter, and the 330K isentropic surface is used in

summer. These surfaces typically lie above the 300 mb level at high latitudes then intersect the tropopause at mid-latitudes and slope down to the 800 mb level at low latitudes. On a daily basis their pattern is modulated by the growth and passage of weather systems. Another useful display is the height of the dynamical tropopause or the so-called "PV=2 surface" (1 PV unit=10^{-6}Kkg^{-1}m^{2}s^{-1}). When the PV=2 height is very low, this means that the tropopause is close to the surface, thus bringing high PV values to low altitudes. In this kind of situation, surface pressure can decrease markedly.

The water vapour satellite imagery, also known as moisture imagery, shows radiance distributions measured in the water vapour absorption band (5.7-7.1 μm) emitted by the Earth-atmosphere system. It has an absorption band centered on the 6.7 μm (Weldon and Holmes 1991). In cloud free conditions the radiance value corresponds to a weighted measure of the atmosphere's net water vapour content in a layer from roughly 500 mb to 250 mb with little contribution from lower levels. The position of contribution function[1] may vary depending on the temperature distribution and the moisture content in the atmosphere.

Some key features of Meteosat water vapour (WV) imagery could have applications in forecasting. The Meteosat WV imagery are derived from the radiation emitted by WV or cloud in the upper or middle troposphere and moist or cloudy regions are represented light shades in contrast to dry regions which are black. Young et al. (1987) discussed a feature in the imagery that leads to intense cyclogenesis: normally the appearance in the water vapour channel of a distinct "dry slot", initially situated to the rear of the cloud head (Böttger et al. 1975, Shutts 1990, Bader et al. 1995), but which overtakes it. Uccellini et al. (1985) noted that pronounced dry (warm) signatures on the imagery represent dry conditions not only near 400 mb level, but throughout a deep layer of the atmosphere extending downward to 700 mb.

We have developed a new method, based on using PV and the Meteosat WV images together, to monitor incipient errors in short range weather forecasts and provide dynamically consistent data to re-run potentially poor forecasts. It will be used

[1] Contribution function describes the contribution of different atmospheric layers to the radiance measured at the satellite (Fischer et al. 1981).

here for testing sensitivity of forecasts to local PV modifications. The following sections describe the method and its applications.

2. THE USE OF PV AND WV IMAGES

2.1 Complementarity of WV images and PV

In the atmosphere, typically an intrusion occurs in association with the development of a low pressure system and cold front on the surface, and a tongue of stratospheric air descends isentropically from high latitudes towards the low latitudes to the west of the northeast-southwest (in the Northern Hemisphere) oriented front. In comparison with the upper tropospheric air, stratospheric intrusions are rich in PV and ozone, deficient in water vapour. The intruding tongue of stratospheric air may generate a structure intermediate in scale between small-scale turbulence on the fringe of the fold and large scale vortex formation (Appenzeller and Davies 1992).

Tropopause "folding" as explained by Reed (1955) can be thought of as a process for detaching and transporting stratospheric air from the main "reservoir" toward the middle troposphere along the axis of the jet streams. The role of tropopause folding in the exchange of air between the stratosphere and troposphere, where the stratospheric air descends into the troposphere is observed by large values of potential vorticity, ozone, and other chemical constituents (Shapiro 1980).

The link between the extruded stratospheric air and cyclogenesis could be established by using the principle of conservation of PV. As stratospheric air subsides into the troposphere, vortex tubes are stretched and static stability decreases noticeably in the lower troposphere. Consequently, absolute vorticity measured on an isentropic surface is generated following parcel trajectories as long as stratospheric values of the PV are preserved. Kleinschmidt (1950 and 1955) mentioned that the advection of a stratospheric reservoir of high PV associated with a low tropopause level is an important element in the development of cyclones. Eliassen and Kleinschmidt (1957)

stated that a disturbance associated with the jet stream is probably responsible for the detached maximum of PV in the lower troposphere during the period of surface cyclogenesis.

An intrusion of dry stratospheric air either due to tropopause folding or breaking can modify the outgoing radiance. This will be observed as a "dark" dry zone (sometimes referred to as "dry slot") in the WV imagery indicating the dry air. In midlatitudes a dry intrusion is marked by a tongue of high PV extending towards the low latitudes from the PV rich stratosphere. In their mature phase stratospheric PV tongues are observed to develop further and then either they curve cyclonically to form a large scale (1000-2000 km) vortex above the surface low (Young et al. 1987), or they curve anticyclonically to form an elongated streamer of stratospheric air (Thorncroft et al. 1993). Some observational studies, such as Uccellini et al. (1985), Keyser and Shapiro (1986) showed that narrow tongues (typically 100-200 km in width) of high PV originate within tropopause folds and could penetrate as low as 700 mb.

Figure (1) presents an example in which PV on the 315K isentropic surface is superimposed on the Meteosat WV image. Dark grey shows dry places, while light grey or white indicates moist zones. Some examples of the relations between the PV and the WV image highlighted above are shown on this figure. For example, around 48-52°N and 30-40°W, the PV maximum (about 7 PVU) coincides with the dry regions (or the "dry slot") of the WV image. The contours of the PV (about 1 PVU), around 50-60°N and 25-40°W, correspond well with the moist regions (or the developing "comma cloud"). Another distinct feature is over the southern part of the UK. In that area, dry air has mixed with the moist air during the maturing phase of the cyclone. The high PV which is about 6-7 PVU is over the dry region. As the PV contours turn cyclonically, they take on the shape of the comma cloud. Other apparent correlations are that the tight PV gradient of the upper troposphere and the low stratosphere are over the regions of the sharp transition zone between the dry and moist/cloudy air on the image. Although it is not shown in this report, similar relations were also found with the PV=2 surface height chart and the WV image of the same day.

In summary, then, during an intrusion event the WV imagery and PV on an isentropic surface are complementary. The dark zone (or the "dry slot") in the WV imagery is a vertically averaged, but horizontally finer scale, visualization of the streamer, while the tongue of stratospheric flow on the isentropic surface is a coarser resolution visualization of the dynamically important PV tracer (Appenzeller and Davies 1992).

2.2 Typical relations between WV image signatures and PV charts

- The dry stratospheric air which is high in PV is seen as a dark region, or the so-called "dry slot", on the water vapour image. There is also a close relationship between the dry regions on the WV image and the high PV values at the rear of a developing cyclone (Appenzeller and Davies 1992, and Young et al. 1987). Other important features are "cloud heads", known to accompany some explosive cyclogenesis events (Bottger et al. 1975, and Shutts 1990).

- The main PV (or PV=2 height) gradient often coincides with the cloud edge/moist boundary, being associated with a front at the upper levels. Frontal cloud forms mostly within the air mass of subtropical origin, and would therefore be expected to be associated with air of low PV. In addition, latent heat release concentrates low PV aloft, shown by the marked edges of the PV distribution on the 315K isentropic surface (or in the height of the PV=2 surface) where the characteristic cyclonic comma clouds are seen.
- The gradient of PV on the 315K isentropic surface (or PV=2 height) tends to be concentrated on the warm side of dark strips associated with the bases of upper troughs, the gradient extends along the cloud edge.

It should be noted that depending on dynamical situations or regions in some cases these relations cannot be seen clearly or may cause misinterpretations:

- If there is a system over the same region for a long time, the related WV image will show dry regions mixed with the moist air. In these situations, the relations described above may not be applied confidently due to complication in the WV imagery.
- Subtropical air may be warm enough to contribute to "dark regions" of the WV image, in spite of the high tropopause, if the upper troposphere is relatively dry. Therefore, "dry slots" in the WV image can appear in these air masses with little or no relation to the PV fields.

2.3 Quality Control and the Intervention Procedure

We compared the UK Meteorological Office Unified model (Cullen 1993) operational short range forecast products of PV charts with the Meteosat WV image on a daily basis. Comparisons between the PV and WV images have the potential to show position errors of PV contours as well as pointing out errors in the intensity of PV distribution (Mansfield 1994, Demirtas and Thorpe 1996). In cases of good analyses, which resulted in good forecasts, PV gradients were large over the distinct dry and moist regions. For some cases, when these kind of relationships were not seen, forecasts were not able to predict the intensity of the observed system. This can also be revealed by comparing the forecast in question with good analyses or better forecasts. PV fields overlain with the imagery can provide verification or cast doubt on the forecast/analyzed position and strength of the intrusions of high PV.

Misfits between the WV image and PV charts can indicate a developing forecast error. In order to correct this error, the next step is to modify the PV distribution over these regions to produce a better match with the WV image (Demirtas and Thorpe 1996). This involves altering the values of PV in the misfit region. By using the invertibility principle for the modified PV distribution one then obtains the related wind and temperature fields. These dynamically consistent new data are then used to provide additional initialization data allowing the re-run of the forecast in question.

In this study, additional wind and temperature data are obtained from non-linear balance PV inversion (Davis and Emanuel 1991, and Ziemianski 1994). Note that the inverted winds are the rotational component of the total wind field. These extra data are then used together with the background data from the original run. [The divergent wind component will be rapidly developed by the prediction model itself.] The additional data are incorporated into the analysis mainly in two parts:

1. Depending on the situation, if there is a lack of PV gradient over a certain location, PV is increased (decreased) over dry (moist) regions. Then, wind and temperature fields of the original forecast are modified.

2. In the case of misplacement or shifts with the WV imagery, PV contours are re-positioned.

The additional data provided from "local PV modifications" are treated as "*bogus observations*" type in the UK Meteorological Office Unified Model (hereafter UM). All data assimilation processes and data quality control are also applied on these extra data. (For details see: Bell et al. 1995, and Ingleby and Parrett 1994.)

The new method just described forms part of the total forecasting system illustrated as a flow chart in appendix 1. Most parts of this system are already automated, except for a few of the most critical interpretive and judgmental tasks. For example, quality control and PV modifications have been manually performed.

3. EXAMPLES OF RE-RUN FORECASTS

The PV-WV method has been applied on real cases (Demirtas, 1996). In the following sub-sections various of these cases will be given.

3.1 Upper Level Sensitivity: 16 February 1995 Case

We study here the rapidly deepening cyclone which developed from a small wave, situated near 40-45°N 35-45°W by 1200 UTC on the 15th February 1995. From 1800 UTC on the 15th to 1800 UTC on the 16th, the central surface pressure of the low decreased from 1007mb to 983mb. This means that pressure deepening was $1mbhr^{-1}$ for 24hrs, the threshold for a so-called bomb event (Sanders and Gyakum 1980). The associated weather observed over the UK on the 16th February 1995 can be given in summary as: rainy, heavy at times particularly from late afternoon onwards, very strong gusty winds, reaching gale force in some places. The forecast from 0000 UTC on the 16th February 1995 did not accurately predict the location and intensity of the system. [Figure 4(a) shows surface pressure differences between the analysis and the forecast. Figure (5) presents tracks of the analysis and the forecast.] It also failed to forecast significant precipitation over many parts of the UK.

3.1.1 PV Modifications

The quality of the 0000 UTC 16th forecast (hereafter FA16) was assessed by comparing its model analysis of PV with the Meteosat WV imagery. It was noted that the PV distribution over the moist regions did not capture well the developing cloud head shape which was situated at 48-52°N 25-15°W at 0000 UTC (figure (2a)). Another apparent misfit is that the tight PV gradient of the tropopause was not over the region of the sharp transition zone between the dry and moist/cloudy air on the image. Although the position of stratospheric high PV (6 PVU), near 52°N 30°W, was situated slightly north of the main dry region (48-50°N 20-28°W), there was not a very large mismatch in that region, but, it did not have the strong PV gradient structure. Therefore, it was concluded that the initial conditions of this forecast poorly represents the observed atmospheric conditions.

3.1.2 Re-run1 Forecast: PV modifications over the dry and moist regions

Local PV modifications were made over the mismatched regions which are indicated in figure (3). The location and the magnitude of distinct PV features were adjusted according to the relation between the WV image and the PV thinking. This step involves increasing upper tropospheric PV values over the "dry slot" and decreasing lower tropospheric PV values over the "cloud head" region. By using the invertibility principle the modified wind and temperature fields are obtained. These dynamically consistent new data are then used to provide additional initialization data allowing the re-run of the FA16 forecast. (In appendix 2, table 1 and table 2 give more details about the re-run1 forecast.)

The new PV distribution was superimposed over the WV image to assess the improved fit of the modified PV (re-run) pattern (figure (2b)). This time dynamically significant features matched with the image in a much better way than for the original forecast. It also better represents the PV gradient over the dry and moist regions which are important key ingredients for the mid-latitude weather systems. In order to see quantitative and qualitative impacts of these PV modifications, the PV inversion products of wind and temperature fields were added to the 0000 UTC run background data and the re-run1 forecast was performed.

Figure (4b) shows differences between the re-run1 forecast and original forecast in terms of their surface pressure at 1000 mb. The PV modification at upper levels resulted in a contribution to the low level cyclonic circulation. The pressure difference between the re-run1 forecast and the analysis is about 1.8 mb at the start of the forecast. When the system arrived over the UK, the pressure difference between the re-run1 forecast and the original forecast is 5 mb at 1800 UTC. Comparing figures (4a) and (4b) implies that the re-run1 forecast compensated for most of the lack of surface development of the original forecast.

Radar images were also compared with this re-run's precipitation prediction (not shown here), and it was found that this run captured the main rainfall regions better than the original forecast. Figure (5) presents trajectories of the analysis (UA16), the re-run1 forecast (RR1), and the original forecast (FA16).

Here we have shown that over the short range, of up to say 2 days ahead, it is possible to use recent advances in dynamical concepts, involving potential vorticity, together with satellite imagery to improve the accuracy of a weather forecast. The re-run1 forecast, based on the application of the new method, predicted the location and intensity of the surface development noticeably better than the original unmodified forecast.

3.1.3 Re-run2 Forecast: PV Modifications over the "cloud head" region

This re-run forecast attempts to incorporate the contribution of PV modifications made only over "the cloud head" region in the FA16 forecast. This involves altering the upper tropospheric PV to match with the WV imagery over the area in question. This re-run forecast will indicate how much these PV features contribute to the surface development. Figure (6) shows the area where upper level PV modifications were made. (In appendix 2, table (1) gives detailed information on the data handling of this re-run forecast. Verification times are as in the table (2)).

Figure 7(a) depicts the modified PV (at 48-53°N, 12-25°W) superimposed over the WV imagery. Although the modifications are not as big as in re-run1, the impact of this re-run forecast is still seen on the surface development. The surface pressure differences between the re-run2 forecast and the original forecast is presented in figure 4(c). It indicates that this re-run resulted in decreasing the surface pressure 2 mb more than the FA16 forecast.

3.1.4 Re-run3 Forecast: PV Modifications over the "dry slot"

The aim of this re-run forecast is to evaluate the impact of PV modifications over the dry regions of the WV imagery. The re-run forecast will elucidate how the upper

tropospheric PV modifications over the WV dry region are attributable to the cyclone development. Figure (8) presents the area where upper level PV modifications were performed. (In appendix 2, table (1) gives information on the data handling. Verification times are as in the table (2)).

Figure 7(b) shows the modified PV (at 20-30°W, 50-53°N) superimposed over the WV image. Results show that this re-run forecast contributed to the surface pressure deepening by 3.7 mb (figure 4(d)).

In summary:

- The FA16 forecast is highly sensitive to the upper level PV modifications,
- The re-run1 forecast which was based on PV modifications over both the "dry slot" and "the cloud head" has compensated for most of the lack of surface deepening in the original forecast,
- The re-run2 forecast which focused on the PV modifications only over the "cloud head" contributed to the surface development but not as much as the re-run1 forecast,
- The re-run3 forecast which involved PV modification only over the "dry slot" implied that the short-range forecast is more sensitive to the PV modifications over the "dry slot" than over the "cloud head".

3.2 Upper Level Sensitivity: 27th April 1992 Case

A cold frontal wave was situated near 40-50°N 20-30°W by 0000 UTC on the 27th April 1992. The cold front wave was first identified on 25 April 1992, as a slow moving system about 1000 km south-east of Newfoundland (Browning et al. 1995). The wave moved in an easterly direction with slight development before deepening 12

mb in 12 hours after 1200 UTC 27 April. The low tracked east-north-eastwards through the English Channel during the night of 27-28 April generating many hours of rain over southern England (Hewson, 1993).

Short-range forecasts (e.g. 48 hours) valid at 0000 UTC on 28th April 1992 predicted incorrectly the position of the low near the UK by up to 300 km. Forecasts of central pressures ranged from 1000 to 1010 mb (Hewson, 1993). A study of this FRONTS '92 IOP3 case revealed that earlier forecasts (0000 UTC and 1200 runs from 26th April 1992) were better than the subsequent forecasts in predicting the synoptic situation at 1800 UTC on the 27th. The later forecast (0000 UTC run from 27th April 1992) was not as successful as the runs from 26th. Comparisons of hand analyses with the model analyses showed that the model analyses were also poor in simulating what happened as described by the additional observations taken on this occasion.

3.2.1 Forecast Quality Control of the System

The quality of the analysis used for the 0000 UTC 27th forecast (hereafter FA27) was assessed by comparing its model analysis of PV charts with the Meteosat WV imagery. It was noted that the PV distribution over the moist regions did not capture well the developing cloud head shape which was situated at 45-50°N, 25-15°W at 0300 UTC (figure 9(a)). Another apparent misfit is the position of stratospheric high PV (at 45-47°N, 30-32°W), which was situated slightly north of the main dry region (45-50°N 30-35°W). The PV contours have not properly captured the shape and position of this feature.

The forecast from the 1200 UTC 26th, (hereafter FC26), seemed to capture the representation of the dry slot better than the forecast from 0000 UTC 27th. This earlier forecast FC26 has larger PV over the dry region (figure 9(b)). Over the moist region, both of the forecasts have not captured fully the cloud head shape. This implies that for this case, the magnitude and position of PV contours are more important over the dry region than the moist region. Comparisons of the PV of the

FC26 forecast and the FA27 forecast suggest that the FC26 forecast can be taken as a reference in order to re-adjust the PV of the poorer FA27 forecast.

3.2.2 Re-run1 Forecast

The role of the upper level PV of the FC26 forecast in providing a better forecast can be examined by "implanting its PV" into the FA27 poorer forecast and comparing this re-run with the original FA27 forecast and the FC26 good forecast.

Local PV modifications of the FA27 forecast initial analysis time were made over the mismatched regions (see figure 10). The modification was introduced by implanting the PV pattern of the FC26 forecast into the PV distribution of the FA27 forecast. (In appendix 2, table (3) presents how this re-run data were handled. Table (4) shows the forecast verification time.)

The re-configured PV pattern on the 315K isentropic surface derived from the LAM analysis field at the start of the forecast is depicted in figure 11(a). The PV modifications at upper levels resulted in a contribution to the low level cyclonic circulation. When the system came close to the UK, the central mean sea level pressure difference between the re-run1 forecast and the FA27 forecast is 4 mb at 1800 UTC 27/4/92. The re-run1 forecast deepened the system 4 mb more than the original forecast (figure 12 (a)). When compared with the FC26 forecast, it was noted that this re-run predicts the pressure minimum 4 mb higher. In conclusion, then, the modifications moved the poorer FA27 forecast about half way towards the better FC26 forecast. (Compare with the figure 12(d).)

3.2.3 Re-run2 Forecast

The wind data provided from the PV inversion model includes only the rotational part of the wind. The re-run forecasts of the previous case and the re-run1 forecast of this case study were all based on the results of the PV inversion model. In this re-run2, since, a posteriori, the good forecast was known and its data were available, wind data were provided from the total wind of the FC26 forecast at 0300 UTC rather than from the PV inversion data. Hence, the re-run2 forecast takes into account both the rotational and divergent parts of the wind. The aim of this re-run forecast is to evaluate and compare the use of the total wind for making re-runs.

The locations of the local PV modifications, which are based on the LAM data taken from the FC26 forecast, are as in figure (10). (In the appendix 2, the details of the re-run3 preparation are as given in table (3). Verification times are as in table (4)). The modified PV pattern on the 315K isentropic surface is presented in figure 11(b): note the marked similarity with the PV pattern for re-run1 in figure 11(a).

The forecast from 27/0000 UTC initialized with the 0300 UTC upper air "extra wind and temperature data", which are provided from the T+27 forecast of the FC26, is closer to the 26/1200 UTC forecast than the original FA27 forecast. The results of the re-run2 forecast showed that using the total wind contributed to the surface pressure deepening by about 5 mb at 1800 UTC 27 April 1992 (figure 12(b)). Comparing this result with the result of the re-run1 implies that using total wind or only the rotational part of the wind does not make a remarkable difference.

3.2.3 Re-run3 Forecast

This re-run is similar to the re-run1 except that the PV of the FC26 forecast over the dry area was increased by about 1 pvu before it was implanted into the FA27 forecast. One of the aims of doing this was to check how this contributes to the forecast. Another aim is to compensate some PV losses which occur due to the data

assimilation process following implantation. Also the PV inversion model sometimes smoothes the PV maximum by about 0.5 pvu. (In appendix 2, other details of the re-run3 preparation are as given in the table (3) which presents data handling. Verification times are as in the table (4)).

Results implied that increasing the upper level PV by 1 pvu contributed to the surface development more than the other re-runs of this case study, even though the data assimilation scheme "smoothed-out" some of the "new data". The results of the re-run3 forecast give the surface pressure minimum to be 1007.6 mb at 1800 UTC 27th April 1992 which is 1.1 mb lower than the re-run1 and 0.3 mb lower than the re-run2 (figure 12(c)). (Compare with the figure 12(d).)

3.3 Low Level Sensitivity: 28th September 1995 Case

Forecasts from 27th and early on the 28th September 1995, valid for 29/1200 UTC, incorrectly brought rain from the Atlantic over southern England. This poor precipitation forecast for the southern UK in the global and the Limited Area Model (LAM) runs was not corrected until the forecast run from 28/1200 UTC. Forecasts improved afterwards due to additional data being provided from the drifting buoys which made a significant impact (Grant et al. 1996). The forecast run from 28/0600 (hereafter FB28) wrongly predicted the existence of the low pressure system over the UK and rainfall. The analysis showed that actually there was a high pressure system and no rain over the UK at 29/1800 UTC.

3.3.1 Forecast Quality Control of the System

The quality of the 0600 UTC 28th September 1995 forecast was assessed by comparing its model analysis of PV with the Meteosat WV imagery. The 330K isentropic surface[2] PV distribution was compared with the WV image at the start of the forecast (figure 13(a)). It was noted that the PV contours had a very slight misfit with the dry and moist/cloudy regions of the WV image (50°N, 30-45°W).

A "trough" of high PV (compared to its background) is located over the isolated dry area. It was expected that the base of the PV trough would coincide with the location of the driest area. There was a slight eastward shift of the PV relative to the WV dry slot. Over the moist/cloudy regions of the WV image, the associated PV contours did not capture well the shape of these regions.

3.3.2 Re-run1 Forecast

This re-run is based on the PV modifications made using guidance from the Meteosat WV image. The aim is to check how the forecast will respond to the local PV re-adjustments at upper levels. In figure (14) the areas of local PV modifications are shown with crosses. They highlight the places where the WV image and the PV distribution do not match well.

The PV modifications were performed only at 200 and 300 mb levels because these are the pressure levels associated with the height of the dynamical tropopause. The "extra data" were also provided only at these levels for re-runs of this case. Another reason for not providing data at other levels is that the current "bogus data" procedures of the UM only allow 1000 points for each run. Therefore, preference was

[2] In this case study PV was displayed on the 330K isentropic surface. The reason is that the choice of the isentropic surface is related with seasonal changes. In midlatitudes in the N. Hemisphere, the 315K isentropic surface is suitable for winter and the 330K isentropic surface is suitable for summer.

given to the levels where PV adjustments were made. (In appendix 2, table (5) gives a brief summary of data handling. Table (6) presents verification times.)

The PV of the re-run 1 was compared with the Meteosat WV image at 28/0600 UTC. There were no apparent misfits between them (figure 13(b). The re-run1 forecast, which was based on this modification, did not make a noticeable impact on the original 28/0600 UTC run forecast. Comparing surface charts of the re-run1 forecast and the FB28 original forecast, it was noted that the pressure patterns were very similar. The difference in the pressure magnitude is about 1 mb, the re-run1 forecast leading to an increase in the central pressure by 1 mb.

The impact of the upper level PV modifications has been investigated in terms of their contributions to the surface development. Although upper level PV adjustments were shown to contribute weakly to the surface development of the low, it did not reduce the deepening as much as implied by the analysis.

3.3.3 Re-run2 Forecast

Our study of the low level PV distributions indicated that there are local maxima of 1.8 PVU at 1000 mb, 1.6 PVU at 900 mb, 1.2 PVU at 800 mb levels at 30-40°W 50-55°N. It is not common to see such high PV maxima at these low levels. Climatological distributions of PV suggest that at mid latitudes in the lower troposphere values of PV are more typically 0.3-0.5 PVU (Hoskins, 1990). These high values might have been created by diabatic processes. The original operational forecast run 28/0600 UTC started with these large PV anomalies, and these might have contributed to the later development. Therefore, the objective of this re-run was to assess the contribution to the system of modifying the low level PV distribution. The associated PV anomalies on the 900 mb, 800 mb, 700 mb and 600 mb were decreased by the order of 1 PVU. In figure (15) the areas of the local PV modifications are shown by crosses. (In appendix 2, table (5) gives a brief summary of data handling.

The verifying time of the original forecast and the re-run2 forecast are as in the table (6)).

Results of the re-run2 forecast showed that the forecast is more sensitive to the PV modifications at lower levels than the upper levels. The upper level PV anomaly may have been of secondary importance in the synoptic scale development of the FB28 forecast. Compared to the FB28 forecast and to the re-run1, the re-run2 with low level PV modifications gave the most beneficial impact, producing significant improvements to the surface pressure and the rainfall over Ireland. Although not shown here, this re-run held back the trough, and rain was consequently only forecast for the southeast of Ireland.

In the experiment in which the magnitude of the diabatically produced low level PV anomalies was decreased, the surface pressure deepening was reduced noticeably. The central pressure difference between the FB28 forecast and the re-run2 is about 8.3 mb at 1800 UTC on the 29th. (Recall that the original FB28 predicted surface pressure maxima 10 mb lower than the analysis.) Comparing figure 16(a) with figure 16 (b) indicates that magnitudes of their central pressure difference and locations are close to each other. The re-run2 forecast is similar to the analysis.

4. SUMMARY AND CONCLUSIONS

This research has used recent advances in dynamical meteorology, involving potential vorticity, together with satellite imagery to assess the sensitivity of short-range weather forecasts to local PV modifications as well as to improve the accuracy of short range weather forecasts. With the use of synoptic examples and sensitivity experiments, processes contributing to the development of extratropical cyclones have been addressed. The discussions have mainly been based on potential vorticity concepts. These provide a vivid view of how on the one hand upper level and low level

processes, and on the other hand physical and dynamical processes, interact with each other during cyclonic developments.

Typical relations between the WV image and PV charts have been derived, and then a new method developed to monitor incipient errors in short range weather forecasts and to provide dynamically consistent data to re-run potentially poor forecasts. In this way dynamical concepts add considerable value to the water vapour data which by themselves would probably not have as significant a forecast impact.

Summary of main conclusions:

- During dry intrusions the WV image and PV on an isentropic surface are complementary. The dry slot in the WV imagery visualizes the streamer, while the tongue of stratospheric flow on an isentropic surface depicts the dynamically important PV tracer.

- Comparisons of Meteosat WV images and PV on an isentropic surface or the height of the PV=2 dynamical surface can be used as a "quality control" tool in operational weather forecasting to validate the model results. Mismatches between the WV image and the PV can highlight potential errors in the initial conditions of the model.

- The method presented in this paper can be used to improve short range weather forecasts. In effect the PV and WV image based approach serves to pin point the location and sub-synoptic scale structure of the upper level features. In cases where the analysis errors occur in the upper troposphere the method can lead to a significant improvement in the short-range forecast skill.

- In cases where the errors were mainly at low levels the method was used as a diagnostic tool. PV anomalies at low levels, generated by local diabatic process, are situated ahead of the upper level PV anomaly and can noticeably influence the system development. This sometimes may cause enhanced pressure deepening at the surface and if poorly analysed can lead to a poor forecast. In the experiment in which the magnitude of the diabatically produced low level PV anomalies was

decreased by 1 PVU, the surface deepening was reduced by around 8 mb, improving the accuracy of the forecast.

- Case studies have shown that modifying PV either at upper levels or at low levels can improve forecasts. Upper/low level PV modifications emphasize the importance of upper and low level data for NWP. The new method can also indicate sensitive regions of the analysis over the Atlantic. (PV modifications were made mostly over the mid-Atlantic). Focusing on predictability studies in terms of PV features, one might better understand the nature of the NWP sensitivity to errors in the initial conditions.

The results described in this paper highlight examples of the sensitivity of short-range weather forecasts to modifications in the tropopause-level potential vorticity distribution. If such modifications can be made in analyses, by using for example satellite imagery, then there is potential for forecast improvement. One could argue that improvements might also accrue by more accurately assimilating the water vapour image data directly into the model initialisation. It is our contention that by using PV concepts we can infer additional data on the atmospheric flow and temperature which cannot be derived simply from the water vapour data. In this way dynamical concepts add considerable value to the water vapour data which by themselves would probably not have as significant a forecast impact.

One can speculate whether such wind and temperature modifications will be automatically produced following the introduction of four-dimensional variational (4DVAR) data assimilation. This is at present unclear as the link between water vapour content and the location of the tropopause is, from the prediction model viewpoint, indirect. Therefore changes to the WV content at the analysis time are likely to take a long time to filter through into consistent wind and temperature changes associated with positional alterations to the tropopause location. The power of the technique used in this paper is that these changes are introduced at analysis time. When 4DVAR is introduced it will be possible to assess these open questions in a systematic way.

It is hoped that the continued application of the quantitative results discussed in this work will yield further insights into the dynamics of synoptic systems and the

nature of the operational weather forecasting. This aims to provide common ground from which observational, numerical, and theoretical work may be easily compared.

ACKNOWLEDGMENTS: Some parts of this paper are taken from the first author's Ph.D. Thesis. We would like to thank Julian Heming at the Met. Office for assisting with re-running the operational forecast. The first author is grateful to the Turkish Ministry of Education for a grant to support these studies.

Appendix 1: A flow chart for the new method.

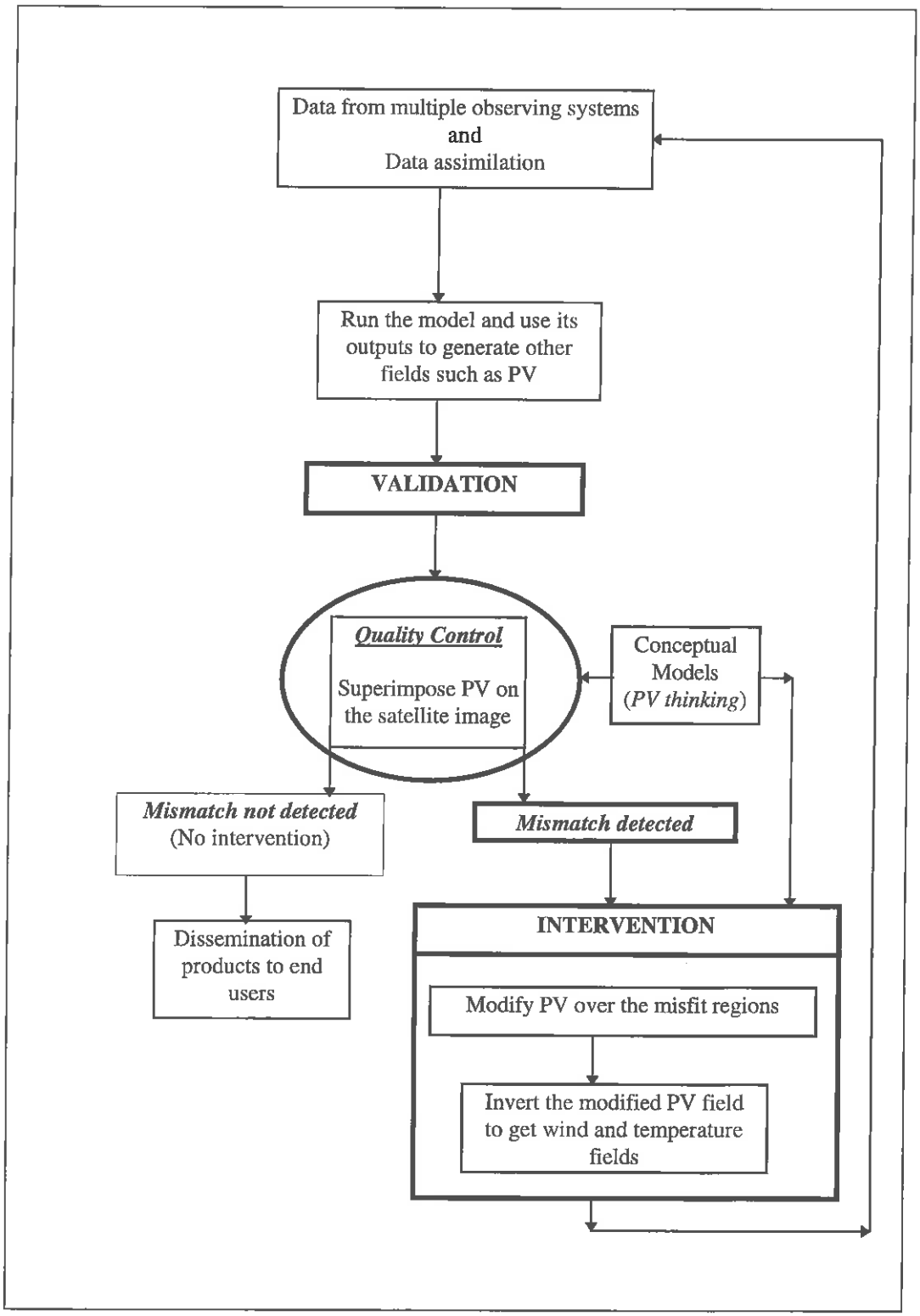

LIST OF TABLES

Table (1): Re-run forecasts data handling details for 16 February 1995 case.

Table (2): Schematic representation of the analysis time, the forecast in question (FA16) and the re-run1 forecast for 16 February 1995 case.

Table (3): Re-run forecasts data handling details for 27 April 1992 case.

Table (4): Schematic representation of the analysis time, the FC26 good forecast, the poorer FA27 forecast in question and the re-run1 forecast for 27 April 1992 case.

Table (5): Re-run forecasts data handling details for 28 September 1995 case.

Table (6): Schematic representation of the analysis time, the forecast in question (FB28) and the re-run1 forecast for 28 September 1995 case.

Appendix 2: Tables of re-runs

Case 1: Re-run forecasts and other details:	
PV modification levels of:	
Re-run1:	***300, 400 and 500 mb***
Re-run2:	***300 mb***
Re-run3:	***300, 400, and 500 mb***
Tools used:	***PV inversion***
Data types:	***Temperature (°C), wind speed (in knots), wind direction (in degrees)***
Data provided at:	***200, 300, 400, 500, and 700 mb levels***
Horizontal resolution of	
Re-run1:	***200 km***
Re-run2:	***200 km***
Re-run3:	***200 km in the x - 100km in the y***
Vertical resolution:	***100 mb***
Total number of points of	***(Locations x data types x levels)=***
Re-run1:	***320***
Re-run2:	***240***
Re-run3:	***80***

Table (1): *Re-run forecasts data handling details for 16 February 1995 case.*

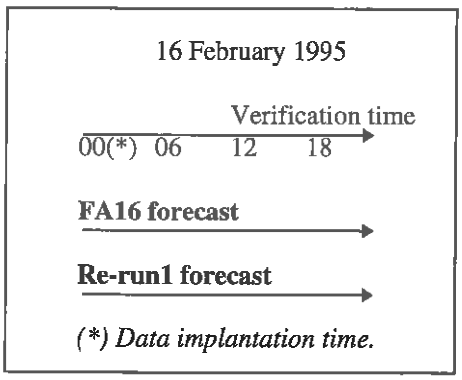

Table (2): *Schematic representation of the analysis time, the forecast in question (FA16) and the re-run1 forecast for 16 February 1995 case.*

Case 2: Re-run forecasts and other details	
PV modification levels:	***300 mb, 400 mb and 500 mb***
Tools used: Re-run1: Re-run2: Re-run3:	 ***PV inversion*** ***LAM data*** ***PV inversion***
Data types:	***Temperature (°C), u (m/s), v (m/s)***
Data provided at:	***300 mb, 400 mb, 500 mb and 700 mb levels***
Horizontal resolution:	***100 km***
Vertical resolution:	***100 mb***
Total number of points:	***(locations x data types x levels)=960***

Table (3): *Re-run forecasts data handling details for 27 April 1992 case.*

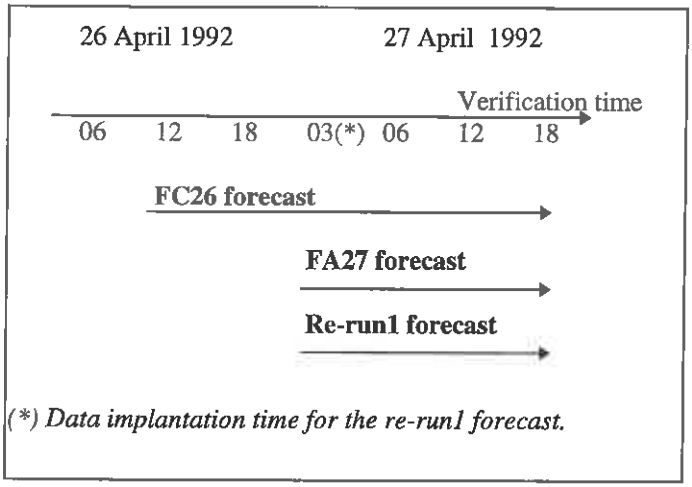

Table (4): *Schematic representation of the analysis time, the FC26 good forecast, the poorer FA27 forecast in question and the re-run1 forecast for 27 April 1992 case.*

Case 3: Re-run forecasts and other details	
PV modification levels of: Re-run1: Re-run2:	 ***200mb and 300 mb*** ***600mb, 700mb and 800mb***
Tools used:	***PV inversion***
Data types:	***Temperature (°C), wind speed (in knots),*** ***wind direction (in degrees)***
Data provided at: Re-run1: Re-run2:	 ***200 and 300mb levels*** ***600, 700, 800 and 900 mb levels***
Horizontal resolution of	***200 km***
Vertical resolution:	***100 mb***
Total number of points of Re-run1: Re-run2:	***(Locations x data types x levels)=*** ***804*** ***800***

Table (5): *Re-run forecasts data handling details for 28 September 1995 case.*

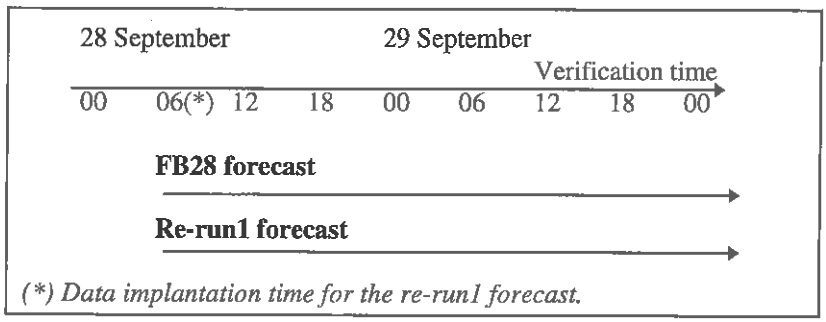

Table (6): *Schematic representation of the analysis time, the forecast in question (FB28) and the re-run1 forecast for 28 September 1995 case.*

References

Appenzeller, C. and Davies, H. C. (1992): Structure of stratospheric intrusions into the troposphere. *Nature*, **358**, 570-572

Bader, M. J. Forbes, G. S., Grant, J. R. Lilley, R. B. E., and Waters, A. J. (1995): Images in the weather forecasting. A practical guide for interpreting satellite and radar imagery. *Cambridge University Press.*

Bell, R. S., Macpherson, B., Robinson, D., and Andrews, P. (1995): Technical details of the Unified Model data assimilation scheme. *Unified Model Documentation Paper* **No. P3**

Böttger, H., Eckardt, M. and Katergiannakis, U. (1975): Forecasting extratropical cyclones with hurricane intensity using satellite information. *J. Appl. Met.*, **14**, 1259-1265

Browning, K. A., Clough, S. A. Davitt, C. S. A., Roberts, N. M., Hewson, T. D. and Healy, P. G. W. (1995): Observations of the mesoscale substructure in the cold air of a developing frontal cyclone. *Q.J.R. Meteorol. Soc.*, **121**, 1229-1254

Cullen, M. J. P. (1993): The Unified Forecast/Climate Model. *Meteorol. Mag.*, **122**, 81-94

Davis, C. A., and Emanuel, K. A. (1991): Potential vorticity diagnostics of cyclogenesis. *Mon. Wea. Rev.* **119**, 1929-1953

Demirtas, M. and Thorpe, A. J. (1996): A new method for short-range weather forecasting - quality control and intervention. *Seventh Conference on Mesoscale Processes, 9-13 September 1996, Reading UK, pp:396-398.*

Demirtas, M. (1996): Sensitivity of Short-Range Forecasts to Local Potential Vorticity Modifications, *PhD Thesis*, University of Reading, *227pp.*

Eliassen, A., and Kleinschmidt, E. (1957): Dynamical meteorology. Handbuch der physik, Vol. **48**, J. Bartels, Ed., Springer-Verlag, 1-154

Fischer, H., Eigenwilling, N. and Muller, H. (1981): Information content of Meteosat and Nimbus/THIR water vapour channel data: altitude association of observed phenomena. *J. Appl. Meteorol.*, **26**, 1655-1670

Grant, J. R., Graham, R. J. and Bader, M. J. (1996): Impact of drifting buoy observations on NWP model evolution - A case study.. *Seventh Conference on Mesoscale Processes, 9-13 September 1996, Reading UK, pp:379-381*

Hewson, T (1993): The FRONTS '92 experiment: A quicklook atlas. *JCMM Internal Report* ***No:15****, University of Reading*

Hoskins, B. J., McIntyre, M. E. and Robertson, A. W. (1985): On the use of and significance of isentropic potential vorticity maps. *Q. J. R. Meteorol. Soc.*, **111**, 877-948.

Hoskins, B. J. (1990): Theories of cyclogenesis. Extratropical cyclones: *The Eric Palmen Memorial Volume, AMS, Boston*, 63-80

Ingleby, N. B. and Parrett, C. A. (1994): Quality control of atmospheric data. Technical documentation. *UK Met. Office, Unified Model Documentation Paper* **P32**

Keyser, D. and Shapiro, M. A. (1986): A review of the structure and dynamics of upper level frontal zones. *Mon. Wea. Rev.*, **114,** 452-499

Kleinschmidt, E. (1955): Die Entstehung einer Höhenzyklone über Nordamerika. *Tellus*, **7,** 96-110

Kleinschmidt, E. (1950): Über Aufbau und Entstehung von Zyklonen (1 Teil). *Meteor. Rundsch.*, **3,** 1-6

Mansfield, D. (1994): The use of potential vorticity in forecasting cyclones, *The International Symposium on the Life Cycles of Extratropical Cyclones,* **Volume III**, 326-331

Reed, R. J., (1955): A study of a characteristic type of upper-level frontogenesis. *J. Meteorol.*, **12,** 226-237

Sanders, F. and Gyakum J. R. (1980): Synoptic-dynamic climatology of the "bomb". *Mon. Wea. Rev.*, **108**, 1589-1606

Shapiro, M. A. (1980): Turbulent mixing within tropopause folds as a mechanism for the exchange of chemical constituents between the stratosphere and troposphere. *J. Atmos. Sci.*, **37,** 994-1004

Shutts, G. J. (1990): Dynamical aspects of the October storm, 1987: A study of successful fine-mesh simulation. *Q. J. R. Meteorol. Soc.*, **116**, 1315-1347

Thorncroft, C. D. Hoskins, B. J. and McIntyre, M. E. (1993): Two paradigms of baroclinic-wave life cycle behaviour. *Q. J. R. Meteorol. Soc.*, **119**, 17-55

Thorpe, A. J. and Bishop, C. H. (1995): Potential vorticity and the electrostatic analogy Ertel-Rossby formulation. *Q. J. R. Meteorol. Soc.* **121**, 1477-1495

Uccellini, L. W., Keyser, D., Brill, K. F., and Wash, C. (1985): The President's Day Cyclone of 18-19 February 1979: Influence of upstream trough amplification and associated tropopause folding on rapid cyclogenesis. *Mon. Wea. Rev.,* **113,** 962-987

Weldon, R. B. and Holmes, S. J. (1991): Water vapour imagery: Interpretation and applications to weather analysis and forecasting. *NOAA Tech: Rep. NESDIS* **57**. US Dept. of Commerce, Washington DC, 213 pp.

Young, M. V. Monk, G. A. and Browning, K. A., (1987): Interpretation of satellite imagery of a rapidly developing cyclone, *Q. J. R. Meteor. Soc.*, **113**, 1089-1115

Ziemianski, M. (1994): Potential Vorticity Inversion, *JCMM Internal Report, **No: 39**, University of Reading.*

LIST OF FIGURES

Figure (1): The Meteosat water vapour imagery in grey shades and the 315K isentropic surface PV in contours at the start of the forecast 0000 UTC on the 24th January 1996. Dark shades represent dry air, light shades represent moist air. (Contour interval is 0.5 PVU.)

Figure (2): The Meteosat water vapour imagery in grey shades and the 315K isentropic surface PV in contours at the start of the forecast 0000 UTC on the 16th February 1995. Dark shades represent dry air, light shades represent moist air. **(a)** is for the original forecast, **(b)** is for the re-run1 forecast.

Figure (3): Locations of the data provided for the re-run1 forecast in the 16 February 1995 case.

Figure (4): Plots for the pressure differences at 1000mb for 1800 UTC. **(a):** The analysis-the FA16 forecast; **(b):** The re-run1 forecast-the FA16 forecast; **(c):** The re-run2 forecast-the FA16 forecast; **(d):** The re-run3 forecast-the FA16 forecast.

Figure (5): The track of the MSLP pressure centres of the analysis (UA16), the re-run1 (RR16) and the original forecast (FA16) shown in dark lines from 0000 UTC on the 16th to 0000 UTC on the 17th 1995.

Figure (6): Locations of the data provided for the re-run2 forecast in the 16 February 1995 case.

Figure (7): As in the figure (2) but for the re-run2 **(a)** and re-run3 **(b)** respectively.

Figure (8): Locations of the data provided for the re-run3 forecast in the 16 February 1995 case.

Figure(9): The Meteosat water vapour imagery in grey shades and the 315K isentropic surface PV in contours at 0300 UTC on the 27th April 1992. Dark shades

represent dry air, light shades represent moist air. **(a)** is for the FA27 forecast at T+3. **(b)** is for the FC26 forecast at T+36.

Figure (10): PV modification locations for the re-run forecasts in the 27 April 1992 case.

Figure (11): As in the figure (9) but for the re-run1 **(a)** and re-run2 **(b)** forecast respectively.

Figure (12): Plots for the pressure differences at 1000mb for 1800 UTC. **(a):** The Re-run1-FA27 forecast; **(b):** The re-run2 forecast-the FA27 forecast;**(c):** The re-run3 forecast-the FA27 forecast; **(d):** The FC26 forecast-the FA27 forecast.

Figure (13): The Meteosat water vapour imagery in grey shades and the 330K isentropic surface PV in contours at the start of the forecast 0600 UTC on the 28th September 1995. Dark shades represent dry air, light shades represent moist air. **(a)** is for the original forecast (FB28), **(b)** is for the re-run1 forecast.

Figure (14): Locations of the data provided for the re-run1 forecast in the 28 September case.

Figure (15): Locations of the data provided for the re-run2 forecast in the 28 September case.

Figure (16): Plots for the pressure differences at 1000mb for 1800 UTC. **(a):** The FB28 forecast-the analysis; **(b):** The FB28 forecast- the re-run2 forecast.

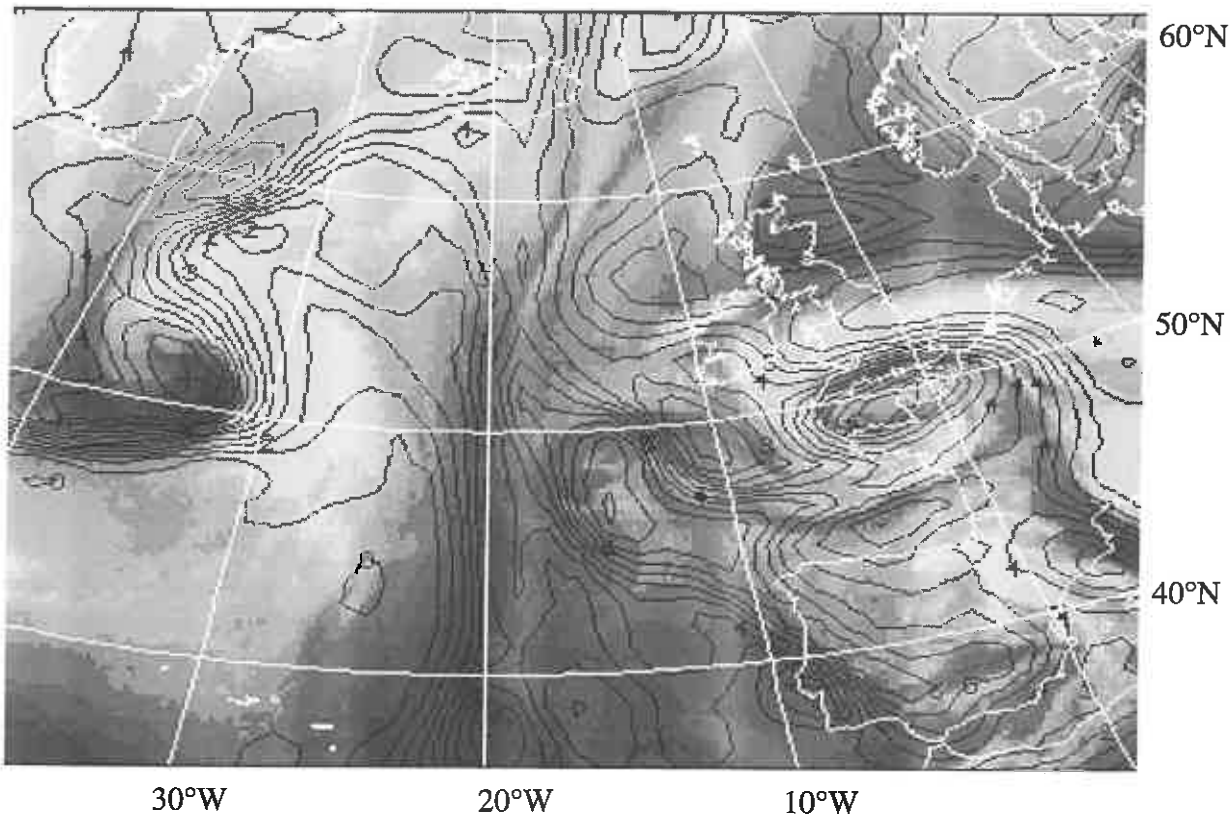

Figure (1): *The Meteosat water vapour imagery in grey shades and the 315K isentropic surface PV in contours at the start of the forecast 0000 UTC on the 24th January 1996. Dark shades represent dry air, light shades represent moist air. (Contour interval is 0.5 PVU.)*

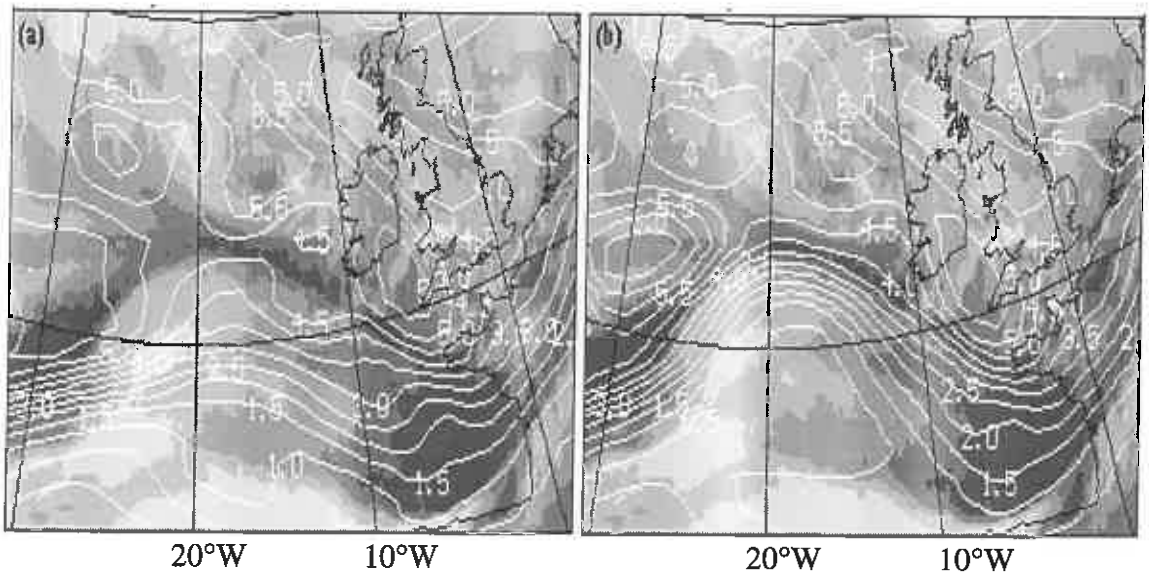

***Figure (2)**: The Meteosat water vapour imagery in grey shades and the 315K isentropic surface PV in contours at the start of the forecast 0000 UTC on the 16th February 1995. Dark shades represent dry air, light shades represent moist air. **(a)** is for the original forecast, **(b)** is for the re-run1 forecast.*

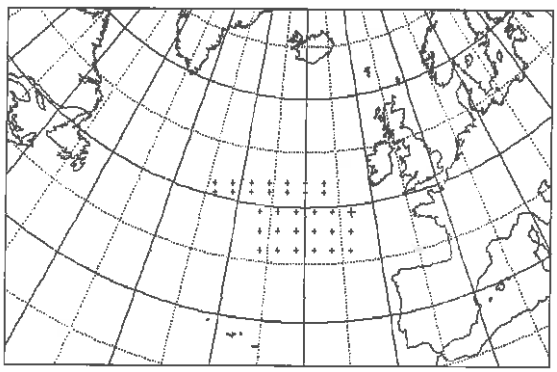

***Figure (3)**: Locations of the data provided for the re-run1 forecast in the 16 February 1995 case.*

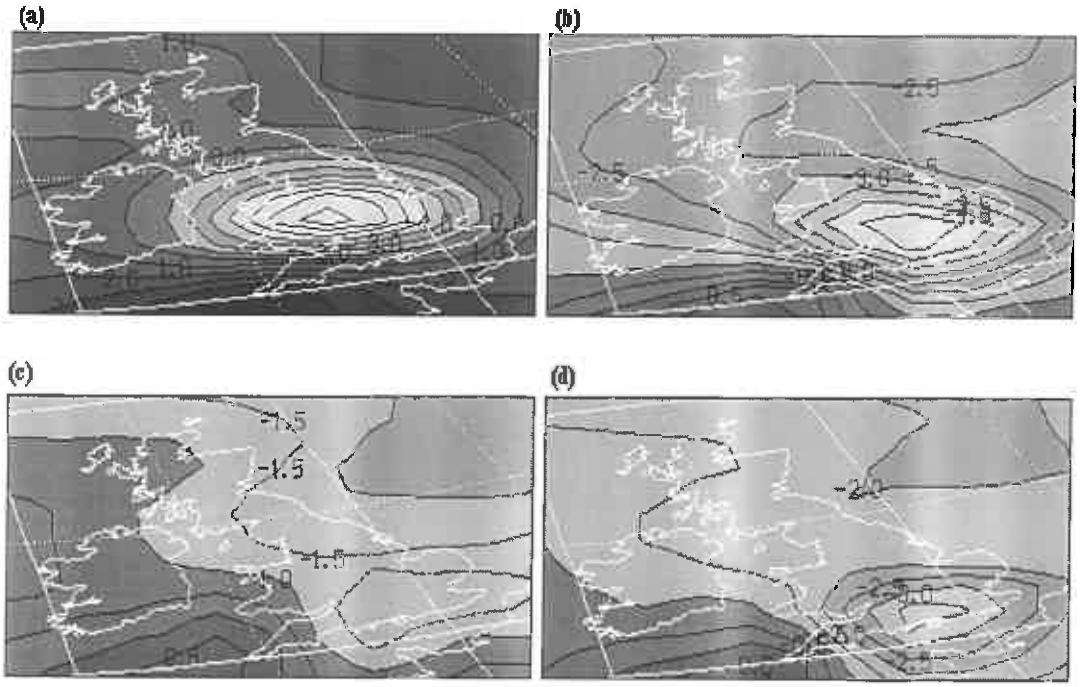

Figure (4): *Plots for the pressure differences at 1000mb for 1800 UTC.* ***(a):*** *The analysis-the FA16 forecast;* ***(b):*** *The re-run1 forecast-the FA16 forecast;* ***(c):*** *The re-run2 forecast-the FA16 forecast;* ***(d):*** *The re-run3 forecast-the FA16 forecast.*

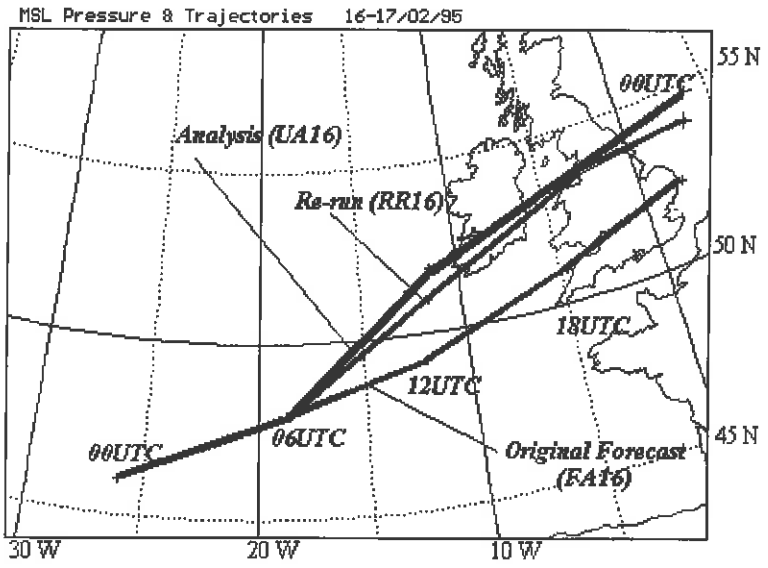

Figure (5): *The track of the MSLP pressure centres of the analysis (UA16), the re-run1 (RR16) and the original forecast (FA16) shown in dark lines from 0000 UTC on the 16th to 0000 UTC on the 17th 1995.*

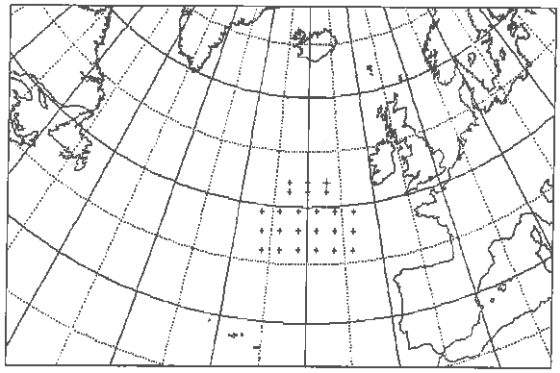

Figure (6): *Locations of the data provided for the re-run2 forecast in the 16 February 1995 case.*

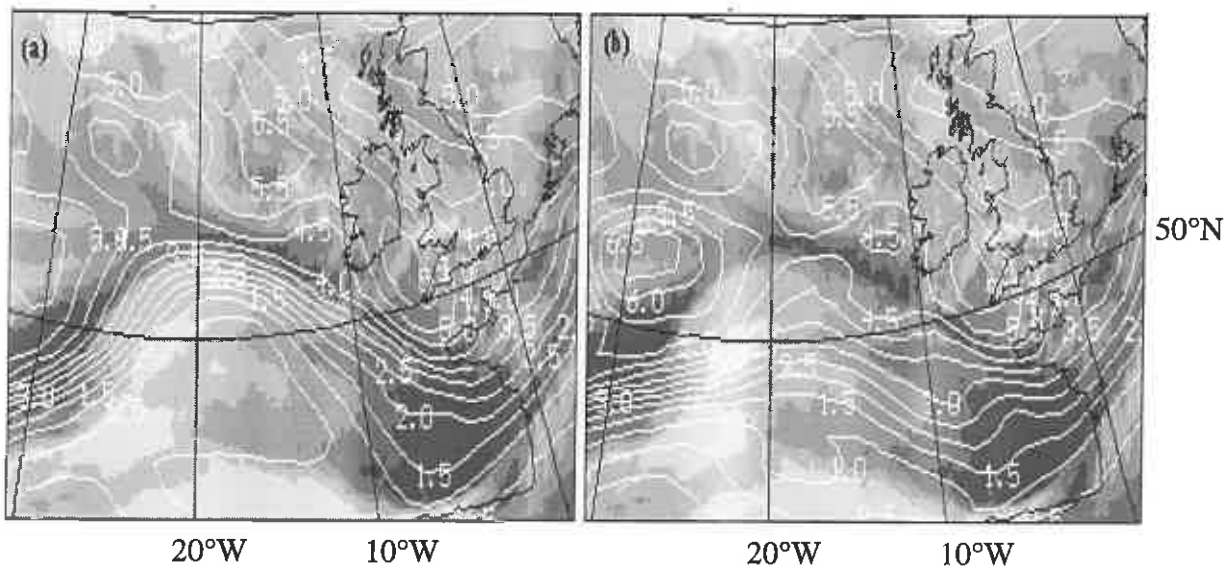

Figure (7): *As in the figure (2) but for the re-run2* ***(a)*** *and re-run3* ***(b)*** *respectively.*

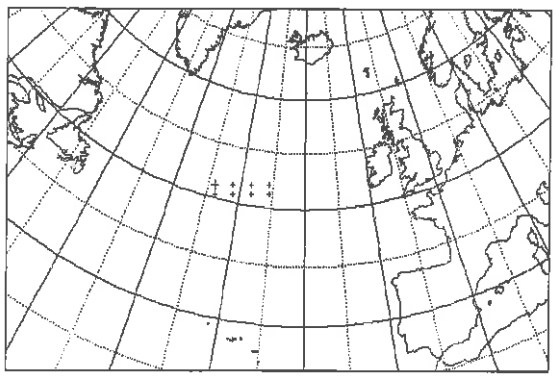

Figure (8): *Locations of the data provided for the re-run3 forecast in the 16 February 1995 case.*

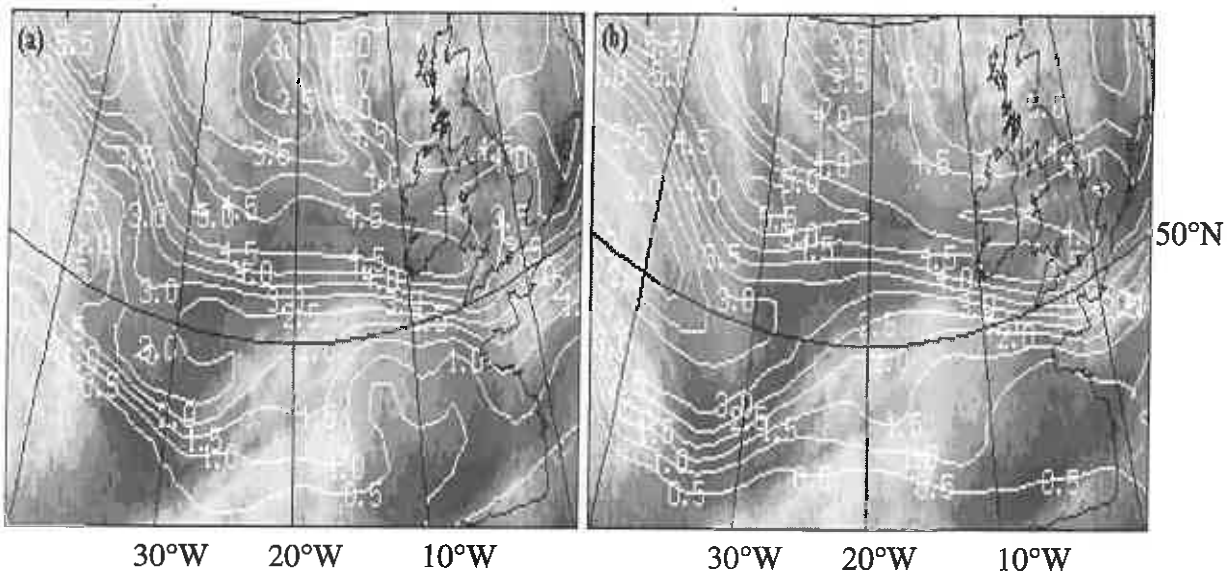

Figure(9): *The Meteosat water vapour imagery in grey shades and the 315K isentropic surface PV in contours at 0300 UTC on the 27th April 1992. Dark shades represent dry air, light shades represent moist air.* ***(a)*** *is for the FA27 forecast at T+3.* ***(b)*** *is for the FC26 forecast at T+36.*

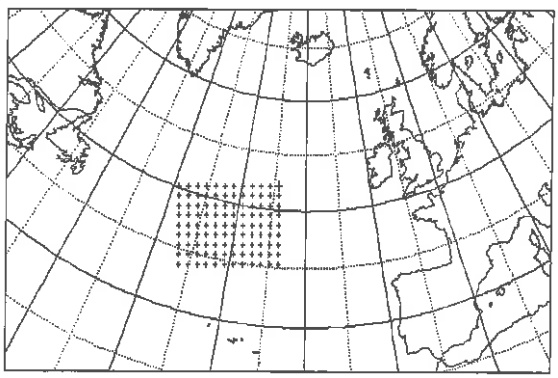

Figure (10): *PV modification locations for the re-run forecasts in the 27 April 1992 case.*

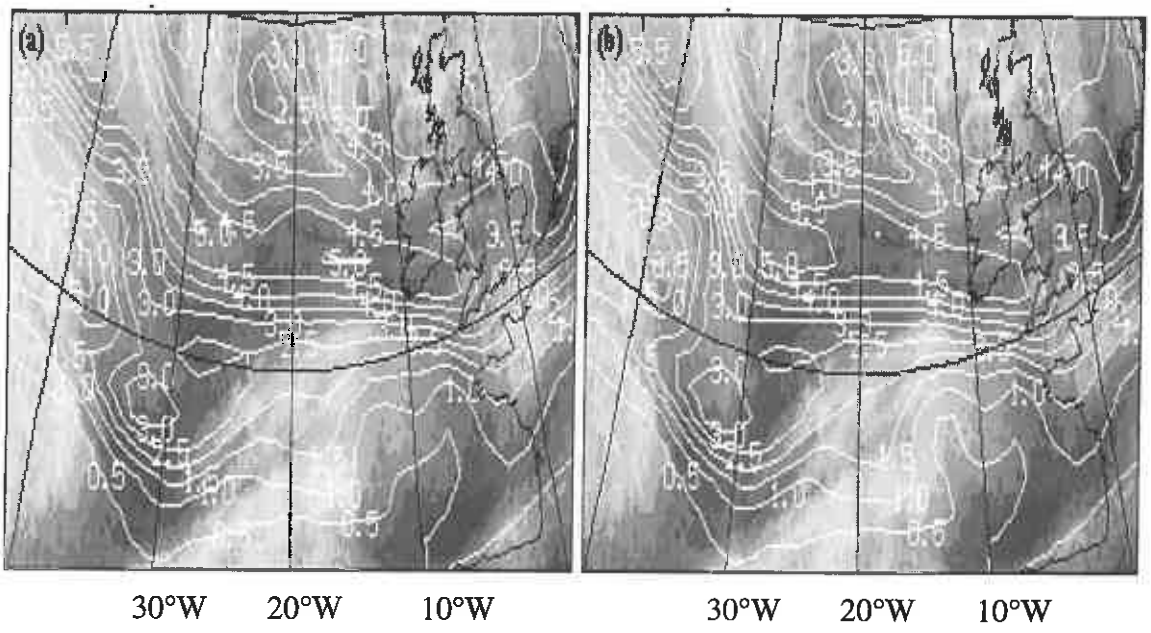

Figure (11): *As in the figure (9) but for the re-run1* ***(a)*** *and re-run2* ***(b)*** *forecast respectively.*

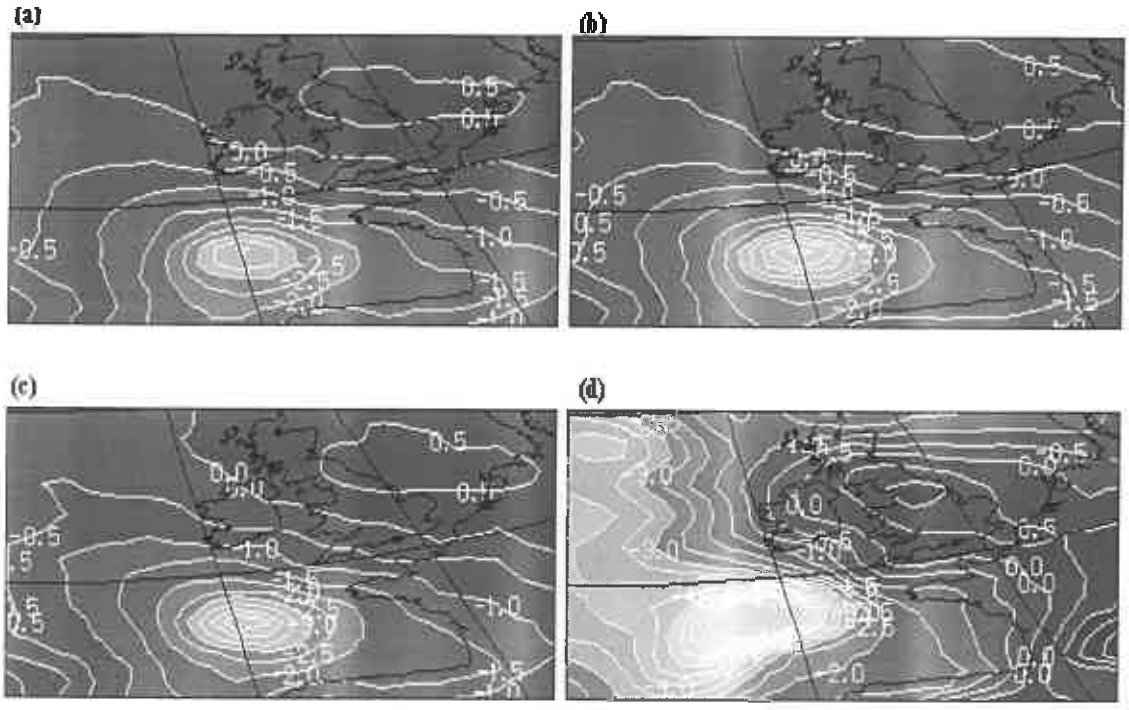

Figure (12): *Plots for the pressure differences at 1000mb for 1800 UTC.* ***(a):*** *The Re-run1-FA27 forecast;****(b):*** *The re-run2 forecast-the FA27 forecast;****(c):*** *The re-run3 forecast-the FA27 forecast;* ***(d):*** *The FC26 forecast-the FA27 forecast.*

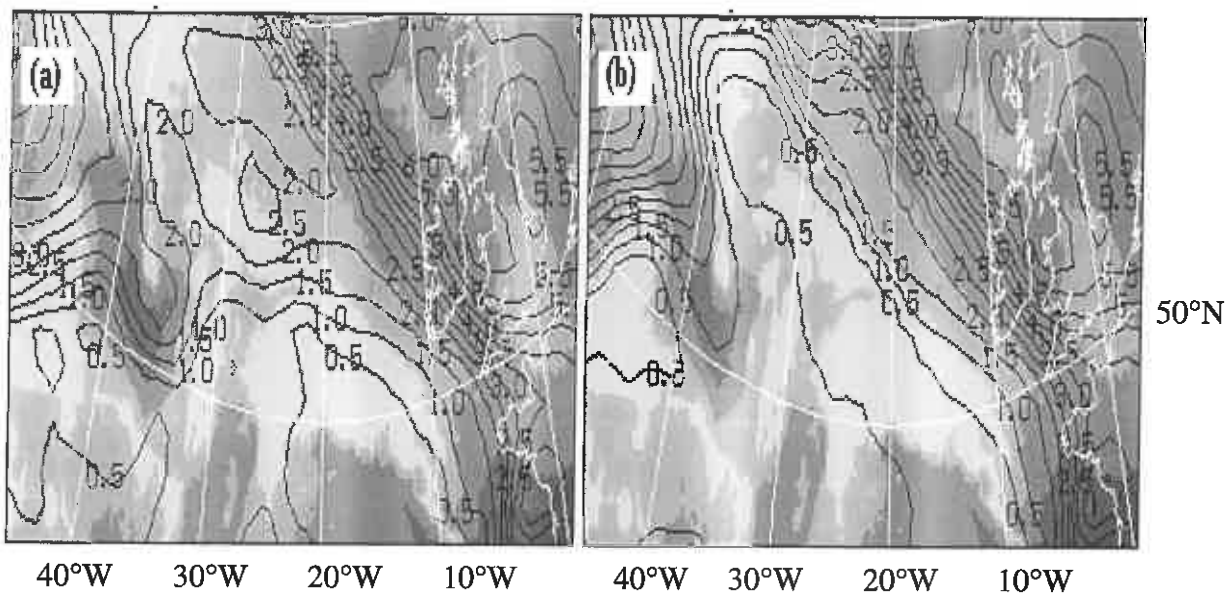

Figure (13): *The Meteosat water vapour imagery in grey shades and the 330K isentropic surface PV in contours at the start of the forecast 0600 UTC on the 28th September 1995. Dark shades represent dry air, light shades represent moist air.* ***(a)*** *is for the original forecast (FB28),* ***(b)*** *is for the re-run1 forecast.*

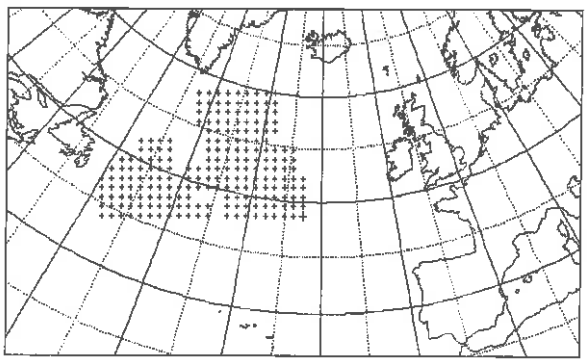

Figure (14): *Locations of the data provided for the re-run1 forecast in the 28 September case.*

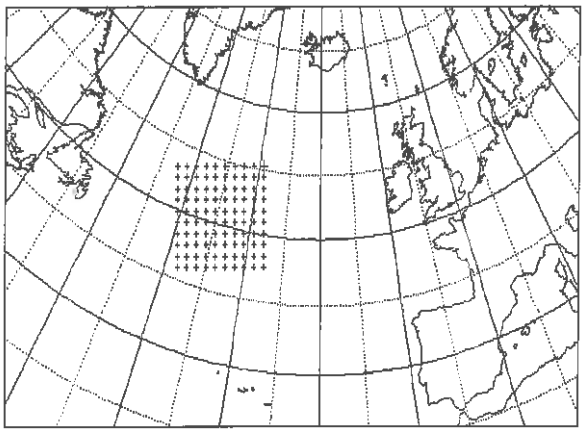

Figure (15): *Locations of the data provided for the re-run2 forecast in the 28 September case.*

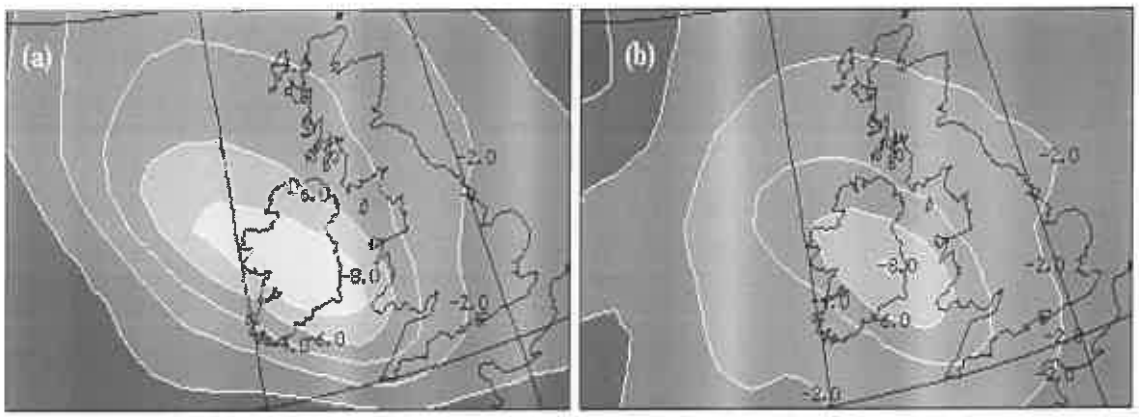

Figure (16): *Plots for the pressure differences at 1000mb for 1800 UTC.* ***(a):*** *The FB28 forecast-the analysis;****(b):*** *The FB28 forecast- the re-run2 forecast.*

CURRENT JCMM INTERNAL REPORTS

This series of JCMM Internal Reports, initiated in 1993, contains unpublished reports and also versions of articles submitted for publication. The complete set of Internal Reports is available from the National Meteorlogical Library on loan, if required.

1. **Research Strategy and Programme.**
   K A Browning et al
   January 1993

2. **The GEWEX Cloud System Study (GCSS).**
   GEWEX Cloud System Science Team
   January 1993

3. **Evolution of a mesoscale upper troposheric voriticity maximum and comma cloud from a cloud-free two dimensional potential vorticity anomaly.**
   K A Browning
   January 1993

4. **The Global Energy and Water Cycle**
   K A Browing
   July 1993

5. **Structure of a midlatitude cyclone before occlusion.**
   K A Browning and N Roberts
   July 1993

6. **Development in Systems and Tools for Weather Forecasting**
   K A Browning and G Szejwach
   July 1993

7. **Diagnostic study of a narrow cold frontal rainband and severe winds associated with a stratospheric intrusion.**
   K A Browning and R Reynolds
   August 1993

8. **Survey of perceived priority issues in the parametrizations of cloud-related processes GCMs**
   K A Browning
   September 1993

9. **The Effect of Rain on Longwave Radiation**
   I Dharssi
   September 1993

10. **Physical Cloud Microphyrocesses - A Description of the Parametrization used in the Large Eddy Model.**
H Swann
July 1994

11. **An Appreciation of the Meteorlogical Research of Ernst Kleinschmidt.**
A J Thorpe
May 1992

12. **Potential Vorticity of Flow Along the Alps**
A J Thorpe, H Volkert and Dietrich Heimann
August 1992

13. **The Representation of Fronts.**
A J Thorpe
January 1993

14. **A Parametrization Scheme for Symmetric Instability: Test for an Idealised Flow.**
C S Chan and A J Thorpe
February 1993

15. **The Fronts 92 Experiment: a Quicklook Atlas**
Edited by T K Hewson
November 1993

16. **Frontal wave satability during moist deformation frontogenesis.**
Part 1. Linear wave dynamics
C H Bishop and A J Thorpe
May 1993

18. **Gravity waves in sheared ducts**
C Bishop and A J Thorpe
November 1993

19. **Potential Vorticity and Electroastatics Analogy: Quasi - Geostrophic Theory.**
C Bishop and A J Thorpe
November 1993

20. **Recent Advances in the Measurement of Precipitation by Radar.**
A J Illingworth - April 1993

21. **Micro-Physique et Givrage. Cloud Microphysics and Aircraft Icing.**
A J Illingworth May 1993

22. **Differential Phase Measurements of Precipitation.**
M Blackman and A J Illingworth
May 1993

23. **Estimation of Effective Radius of Cloud Particles from the Radar Reflectivity**.
N I Fox and A J Illingworth
May 1993.

24. **A Simple Method of Dopplerising a Pulsed Magnetron Radar**.
A Hau, A J Illingworth and J Eastment
November 1993.

25. **Radiation and Polar Lows.**
George C Craid
February 1994

26. **Collected preprints submitted International Symposium on the life Cycles of Ectratropical Cyclones; Bergen, Norway, 27 June - 1 July 1994**
April 1994.

27. **Convective Frontogenesis**
Douglas J Parker and Alan J Thorpe
April 1994

28. **Improved Measurement of the Ice Water Content in Cirrus Using a Total Water Evaporator.**
Philip R A Brown and Peter N Francis
April 1994

29. **Mesoscale Effects of Dry Intrusion within a vigorous Cyclone**
K A Browning and B W Golding
April 1994

30. **GEWEX Cloud System Study, Science Plan**
May 1994

31. **Parametrization of Mometum Transport by Convectively Generated Gravity Waves.**
R Kershaw
February 1995

32. **Mesoscale Modelling Newsletter, No5.**
May 1994

33. **Observations of the mesoscale sub-structure in the cold air of a developing frontal cyclone.**
K A Browning, S A Clough, C S A Davitt, N M Robertsf and T D Hewson
May 1994

34. **Longwave Radiative Forcing of a Simulated Tropical Squall Line**
Imtiaz Dharssi
July 1994

35. **On the nature of the convective circulation at a Kata-cold front**
K A Browning
September 1994

36. **Collective preprints of papers submitted to the COST-75 International Seminar on Advanced Weather Radar Systems, Brussels, 20-23 September 1994.**
November 1994

37. **Use of satellite imagery to diagnose events leading to frontal thunderstorms: Parts 1 and 11 of a case study.**
K A Browning and N M Roberts
November 1994

38. **The role of spaceborne millimeter-wave radar in the global monitoring of ice cloud.**
P R A Brown, A J Illingworth, A J Heymsfield, G M McFarquahar, K A Browning and M Gosset.
December 1994

39. **Potential Vorticity Inversion**
Michael Ziemianski
October 1994

40. **Theory of mature tropical cyclones; A comparison between Kleinschmidt (1951) and Emanual (1986)**
Suzanne L Gray
December 1994

41. **Dispersion and removal of pollutants during the passage of an atmospheric frontal System.**
N R Gimson
December 1994

42. **The role of snow sublimation in frontogenesis**
D J Parker and A J Thorpe
December 1994

43. **Potential vorticity and the electrostatics Analogy: Ertel- Rossby formulation**
A J Thorpe and C H Bishop
December 1994

44. **Mesoscale aspect of extratropical cyclones: and observational perspective**
K A Browning
January 1995

46. **Generation of near-surface gusts of deep convection**
K Nakamura and R Kershaw
April 1995

47. **Attribution concepts applied to the Omega Equation**
S A Clough, C S A Davitt and A J Thorpe
June 1995

48. **Parametrization of mixed-phase cloud and precipitation**
Susan P Ballard and M Gerard Hutchinson
June 1995

49. **Short-range forecasting of stratocumulus: Initialization V Prediction**
Susan Ballard, Simon D Jackson and B Macpherson
June 1995

50. **Contribution of the JCMM/Dept of Meteorology Radar Group to the 27th AMS Radar Meteorology Conference, Vail October 1995.**
June 1995

51. **Cold pools in shear**
Douglas J Parker
September 1995

52. **High-resolution analysis of frontal fracture**
K A Browning, S P Ballard and C S A Davitt
September 1995

53. **The Albedo of Broken Cloud Fields: Calculations using a modified two stream radiation code.**
Imatiaz Dharssi and Roy Kershaw
October 1995

54. **Parametrization of momentum transport by convection. I: Theory and cloud modelling results.**
P Kershaw and D Gregory
November 1995

55. **Variation of frontal structure along a cold front**
K A Browning and N M Roberts
November 1995

56. **Secondary Frontal Waves**
Douglas Parker
December 1995

57. **Objective Fronts**
T D Hewson
March 1996

58. **Mesoscale analysis of the activation of a cold front during cyclogenesis**
K A Browning, N M Roberts and A J Illingworth
June 1996

59. **Investigation of different representations of rain in a 1-d evaporation model**
H Swann
May 1996

60. **Parametrization of diabatic processes in the inversion of the omega-equation**
M Athanassiadou and A J Thorpe

61. **The role of the environmental flow in the development of secondary frontal cyclones.**
I A Renfrew, A J Thorpe and A Joly
June 1996

62. **Contributions to the AMS/RMS Conference on Mesoscale Processes Reading**
S Malardel, A J Thorpe and A Joly
June 1996

63. **Contributions to the AMS/RMS Conference on Mesoscale Processes Reading**.
9-13 September 1996
June 1996

64. **Vorticity and Potential Vorticity Stratified Flows Interacting with an Isolated Obstacle.**
Jorge A Gutierrez and A J Thorpe - September 1996

65. **Triple Point Development: Two Case Studies**
Douglas Parker
September 1996

66. **Radar observations of wind-shear splitting within evolving atmospheric Kelvin-Helmholtz billows**
D. Chapman and K.A.Browning
April 1997

67. **Cold Frontal Structure derived from radar wind profilers**
K.A.Browning, D. Jerrett, J.Nash, T.Oakley, N.M.Roberts
May 1997

68. **The dry intrision and its effect on the frontal, cloud and precipitation structure of extratropical cyclones**
K.A. Browning - Text of invited special lecture at the Spring Conference of the Meteorological Society of Japan, University of Tsukuba, 22 May 1997.

69. **Met. Office Unified Model data, diagnostic, graphics programs, and other observational data available from the JCMM through the aegis of the Universities Weather Research Network UWERN**. Plus supplement.
Peter Panagi and Ed Dicks
June 1997

70. **Contributions of the JCMM/Dept of Meteorology Radar Group to 28th AMS Radar Meteorology Conference.** Austin, Texas, September 1997

71. **Sensitivity of short-range weather forecasts to local potential vorticity modifications.**
Meral Demirtas and Alan Thorpe.
July 1997.

Met Office Joint Centre for Mesoscale Meteorology Department of Meteorology
University of Reading PO Box 243 Reading RG6 6BB United Kingdom
Tel: +44 (0)118 931 8425 Fax: +44 (0)118 931 8791
www.metoffice.com